Autochthonous organic matter promotes DNRA and suppresses N2O production in sediments of the coastal Baltic Sea

Aalto, Sanni L.

2021-07-05

1 Autochthonous organic matter promotes DNRA and suppresses N_2O

2 production in sediments of the coastal Baltic Sea

3 Sanni L. Aalto[1,2*], Eero Asmala[3], Tom Jilbert[3,4], Susanna Hietanen[3,4]

4 [1]Department of Environmental and Biological Sciences, University of Eastern Finland, P.O. Box 1627,
5 70211 Kuopio, Finland

6 [2]Department of Biological and Environmental Science, University of Jyväskylä, P.O. Box 35, 40014
7 Jyväskylä, Finland

8 [3]Tvärminne Zoological Station, University of Helsinki, 10900 Hanko, Finland

9 [4]Ecosystems and Environment Research Program, Faculty of Biological and Environmental Sciences,
10 00014 University of Helsinki, Helsinki, Finland

11 Corresponding author: Sanni L. Aalto, sheaa@aqua.dtu.dk

12 *current address: Technical University of Denmark, DTU Aqua, Section for Aquaculture, The North Sea
13 Research Centre, P.O. Box 101, DK-9850 Hirtshals, Denmark

14 Abstract

15 Coastal environments are nitrogen (N) removal hot spots, which regulate the amount of land-derived
16 N reaching the open sea. However, mixing between freshwater and seawater creates gradients of
17 inorganic N and bioavailable organic matter, which affect N cycling. In this study, we compare nitrate
18 reduction processes between estuary and offshore archipelago environments in the coastal Baltic Sea.
19 Denitrification rates were similar in both environments, despite lower nitrate and carbon
20 concentrations in the offshore archipelago. However, DNRA (dissimilatory nitrate reduction to
21 ammonium) rates were higher at the offshore archipelago stations, with a higher proportion of
22 autochthonous carbon. The production rate and concentrations of the greenhouse gas nitrous oxide
23 (N_2O) were higher in the estuary, where nitrate concentrations and allochthonous carbon inputs are
24 higher. These results indicate that the ratio between nitrate and autochthonous organic carbon
25 governs the balance between N-removing denitrification and N-recycling DNRA, as well as the end-
26 product of denitrification. As a result, a significant amount of the N removed in the estuary is released
27 as N_2O, while the offshore archipelago areas are characterized by efficient internal recycling of N. Our
28 results challenge the current understanding of the role of these regions as filters of land-to-sea
29 transfer of N.

30 Keywords: denitrification; DNRA; DOM; estuary; N_2O; sediment organic matter

1 Introduction

Coastal systems are transitional zones where riverine freshwater mixes with saline seawater. They are important hot spots in the nitrogen (N) cycle, as N transformations in coastal ecosystems regulate the amount of land-derived N reaching the open sea (Bouwman et al., 2013). Various coastal processes, including assimilation to biomass and subsequent microbial degradation of organic matter, modulate land-to-sea transfer of N. Crucially, N may be removed from biogeochemical cycling in estuaries by a sequence of sedimentary microbial processes terminating in denitrification, which releases dinitrogen gas (N_2) into the atmosphere. Denitrification is a critical part of the 'coastal filter'; the set of biogeochemical processes regulating the impact of riverine nutrient inputs on coastal eutrophication (Asmala et al., 2017).

Denitrification rates in coastal environments depend on nitrate concentrations, which typically decrease from near-shore to offshore areas (Asmala et al., 2017). However, heterotrophic denitrification also depends on the presence of bioavailable organic carbon (OC) in coastal sediments (Hellemann et al., 2017; Hietanen and Kuparinen, 2008). Higher OC bioavailability has been suggested to promote denitrification in freshwater stream sediments (Barnes et al., 2012; Stelzer et al., 2014), raising the question of whether the same is true in coastal marine systems. Coastal systems often display strong gradients in both nitrate concentrations, and in sedimentary OC sources and characteristics, with distance away from river mouths. Typically, the relative amount of terrestrial OC in sediments decreases gradually along the coastal salinity gradient, while the amount of fresh, autochthonous phytoplankton-derived OC increases (Fellman et al., 2011; Goñi et al., 2003; Spencer et al., 2007). Combined, these observations suggest that coastal nitrate removal efficiency through denitrification could be related to the availability of both nitrate and bioavailable OC (Asmala et al., 2017).

The balance in the availability of nitrate and bioavailable carbon may also influence rates of alternative nitrate reduction pathways. Heterotrophic dissimilatory nitrate reduction to ammonium (DNRA), which retains N as biologically reactive ammonium in the aquatic system (e.g., Giblin et al., 2013), is the prominent pathway under conditions of high OC availability relative to nitrate (Hardison et al., 2015; Kraft et al., 2014). This phenomenon may occur because under nitrate-limited conditions, DNRA makes more efficient use of the available electron acceptors (6 electrons transferred per mole of N reduced compared to 3 for denitrification), and therefore maximizes entropy production (Algar and Vallino 2014). Furthermore, OC composition is as important as OC availability in controlling the nitrate reduction end-product (Carlson et al., 2020). From this, it follows that the importance of DNRA in net nitrate reduction may increase towards the open sea where terrestrial influence decreases (lower nitrate and higher bioavailable carbon concentrations). Indeed, high contributions of DNRA to total nitrate reduction were

64 recently observed in the Baltic Sea offshore region (Hellemann et al., 2020) and in Australian estuaries

65 (Kessler et al., 2018). Therefore, outer coastal areas may recycle nitrate more efficiently than remove it, in

66 comparison with near-shore areas with a lower bioavailable OC to nitrate ratio, which favours

67 denitrification.

68 Incomplete denitrification leads to the production of nitrous oxide (N_2O). The proportion of N_2O production

69 from total denitrification can increase with DIN concentrations (Murray et al., 2015), and decrease with

70 increased bioavailable carbon (Zhao et al., 2014). This suggests that among other variables (e.g. oxygen,

71 temperature, salinity, and rates of nitrogen fixation and nitrification; Foster and Fulweiler, 2016;

72 Silvennoinen et al., 2008; Zhao et al., 2014), OC bioavailability is an important factor controlling

73 denitrification-derived N_2O production in coastal ecosystems, and N_2O production the rates may be higher

74 in near-shore estuarine environments with low amounts of bioavailable OC and high nitrate

75 concentrations. Hence, OC characteristics and especially bioavailability may play a key role in many

76 aspects of coastal sedimentary N cycling. These factors must be deconvolved from the effects of

77 nitrate gradients to properly understand the coastal N cycle.

78 The overall bioavailability of aquatic OC can be assessed with optical proxies of dissolved organic

79 matter (DOM), derived from the absorbance and fluorescence properties of the colored dissolved

80 organic matter (CDOM) (Asmala et al., 2013). A range of optical proxies (e.g. the humification index

81 (HIX) and the index of recent autochthonous contribution (BIX)) have been derived to characterize the

82 DOM pool (Huguet et al., 2009; Murphy et al., 2008). We assume DOM in sediment porewaters to

83 reflect the broad overall organic matter composition of sediments, and optical analysis of porewater

84 DOM composition provides a tool for characterizing the source and bioavailability of sedimentary

85 carbon. Porewater DOM characterization potentially provides additional information to traditional

86 approaches such as C/N ratios or $\delta^{13}C$ of bulk organic matter.

87 Here, we investigate the combined influence of nitrate availability and organic matter composition on

88 nitrate reducing processes in coastal sediments in the northern Baltic Sea. The Baltic is a semi-enclosed

89 shallow brackish water basin with significant anthropogenic N loading. In 2010, the total N load to the Baltic

90 was 977 000 tons, of which 758 000 tons was waterborne (Helcom 2015), yielding a waterborne N load

91 from the catchment of 0.44 tonnes/km². The Baltic Sea coastal zone (29% of total Baltic Sea area) was

92 estimated to remove 16% of land-derived N inputs, the N removal efficiency varying between different

93 types of coastal ecosystems (Asmala et al. 2017). Denitrification dominates N_2 production in Baltic Sea

94 coastal ecosystems, with anammox playing only a minor role (Bonaglia et al., 2014; Hietanen, 2007;

95 Thamdrup and Dalsgaard, 2002). Knowledge on the balance between denitrification and DNRA is limited

96 for this region, but results from an anthropogenically impacted Baltic Sea estuary suggest that

97   denitrification is the main process (Bonaglia et al., 2014) due to the high DIN availability, and that the

98   contribution of DNRA increases to 30-50% of total nitrate reduction in the offshore region (Hellemann et

99   al., 2020). The limited data from oligotrophic coastal sediments of the Baltic Sea, where availability of labile

100 organic carbon limits the denitrification process, also indicate that N_2O production from benthic

101 denitrification is low ($N_2O:N_2$ <0.02) (Hellemann et al., 2017).

102 In this study, we measured porewater DOM characteristics, nitrous oxide concentrations, and N

103 processes along a gradient encompassing near-shore (estuary) and offshore archipelago stations in a

104 coastal region of the Baltic Sea to examine the effects of both nitrate availability and OC characteristics

105 on nitrate reduction processes. We hypothesized that higher nitrate availability and terrestrial

106 dominance of the carbon pool (i.e. low quantities of bioavailable carbon compared to nitrate) would

107 promote denitrification and possibly N_2O production at the near-shore estuarine stations. Conversely,

108 we hypothesized that the significance of DNRA as a nitrate reduction process would increase at the

109 offshore archipelago stations due to a higher amount of bioavailable carbon and/or lower nitrate

110 concentrations.

2   Materials and methods

### 2.1   Study area, sampling, and water column analyses

113 The study was conducted in the Finnish coastal area of the Gulf of Finland, Baltic Sea.

114 Pohjanpitäjänlahti is a long and narrow embayment that receives freshwater input from the river

115 Mustionjoki and brackish water input from the adjacent coastal archipelago of the Baltic Sea (Fig. 1).

116 A shallow (2-3 m) sill area, with a dredged 6 m channel through it, separates the estuary from the

117 offshore region connecting to the open Baltic Sea, limiting the water exchange between the estuary

118 and the offshore region. The inner basin is salinity-stratified, with a pronounced pycnocline at 10-15

119 m water depth, which leads to seasonal hypoxia in summer and autumn. Inflows of brackish water

120 over the sill usually occur in late autumn – early winter, leading to temporary ventilation of the basin

121 (Malve et al., 2000). The adjacent offshore region experiences temperature stratification in summer,

122 leading to the development of hypoxia in isolated areas. However, much of that remains oxic

123 throughout the annual cycle due to sufficient vertical mixing and exchange of water masses. The

124 catchment of the Mustionjoki has a large proportion of lakes (11%; Mattsson et al., 2005) and several

125 hydropower plants regulating the flow. This characteristic leads to extensive processing of the riverine

126 nutrients and organic matter already within the lotic system and relatively low area-specific loading

127 of organic carbon to the estuary (Räike et al., 2012).

128   To monitor water column N_2O concentrations, water column sampling was conducted at stations P4

129   ("estuary", see Fig. 1) and STF ("offshore archipelago") at 5 m depth intervals using a 5L Limnos

130   sampler on multiple occasions during 2015-2017. Subsamples for determination of dissolved N_2O

131   were collected in triplicate by filling 60mL plastic syringes directly from a Limnos water sampler on

132   board. In the laboratory, the water volume in the syringe was reduced to 30 mL, and 31mL of 5.0 purity

133   N2 gas was injected to create a headspace. Syringes were left at 20 C for 30 min and then vigorously

134   shaken for 3 min, after which 25mL of the headspace was injected into a pre-evacuated 12mL gastight

135   glass vial (LabCo Exetainer model 839W). Nitrous oxide concentrations in the headspace were

136   determined using an Agilent Technologies 7890B gas chromatograph equipped with electron capture

137   detector (ECD) and the results calculated as in Myllykangas et al. (2017).

138   Sampling was carried out at two stations in the estuary (stations P1 and P4) on 6th of June 2017 and

139   15th–16th of August 2017 and at two stations in the offshore archipelago region (stations P10 and STF;

140   Fig. 1) only on 15th–16th of August 2017. Sampling occasions were chosen to represent situations with

141   high (June) and low (August) amount of fresh, recently deposited phytoplankton-derived material on

142   the sediment surface (Heiskanen and Kononen, 1994). Temperature, salinity and oxygen were

143   determined using a YSI CTD equipped with an optical oxygen sensor. Sediment cores were collected

144   using a Gemax twin sampler (core diameter 9 cm, length of a core 30 - 50 cm) from each sampling

145   station. Water samples were collected using a 5L Limnos water sampler from 1 m depth to 1 m above

146   the sediment at 2-5 m intervals, and from the overlying water of the sediment cores. Oxygen samples

147   for Winkler titration (150 ml) were treated immediately with fixing reagents and analyzed the

148   following day. Dissolved inorganic nitrogen (ammonium, nitrite and nitrate) samples were collected

149   in acid-washed plastic bottles, filtered through 0.2µm polycarbonate filters and stored dark at 4°C.

150   Concentrations were measured using a discrete photometric analyzer (Thermo Scientific Aquakem

151   250) the following day. Theoretical 3-sigma detection limits were as follows: ammonium 0.11 µM,

152   nitrate and nitrite 0.08 µM.

153   Figure 1. (left) Sampling locations in the Pohjanpitäjänlahti system on the Finnish coast of the Gulf of
154   Finland, northern Baltic Sea. Stations P1 and P4 are classified as "estuary" stations, while P10 and STF
155   are classed as "offshore archipelago". The Mustionjoki river discharges into the Pohjanpitäjänlahti
156   estuary close to station P1. (right) Bathymetric detail of the transect through the sampling locations,
157   showing typical salinity distribution (data shown here from June 2015, redrawn from Jilbert et al.,
158   2018). A shallow sill close to the city of Ekenäs restricts exchange of brackish deeper waters between
159   the offshore archipelago and estuary.

160
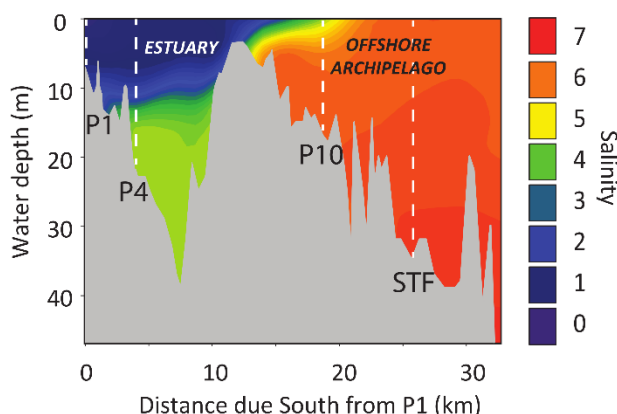
2.2 Sediment and porewater analyses

Sediment cores were collected using a Gemax twin sampler (core diameter 9 cm, length of core 30 - 50 cm) from each sampling station. Sediment water content and porosity were determined from the upper portion of each core (0–6 cm) (Burdige, 2006). Sediment total C and N content (%C, %N) of the upper portion was determined by Thermal Combustion Elemental Analysis (TCEA) at Tvärminne Zoological Station with precision and accuracy of < 2.5% RSD. Sedimentary inorganic carbon and nitrogen are assumed insignificant in this setting, hence $\%C_{tot}$ and $\%N_{tot}$ are assumed equal to organic carbon and nitrogen, respectively ($\%C_{org}$ and $\%N_{org}$).

Porewater DOC and CDOM samples were taken from the surface sediment layer (0-1 cm) of three replicate cores. In the laboratory, pore water was extracted with centrifuging (1500 rpm for 10 min), and filtered through a combusted (4 h 450 °C) glass fiber filter (47 mm, VWR collection GF/F). DOC concentration in porewaters was measured with a Shimadzu TOC-V_{CPH} analyzer. The detection limit for DOC analysis was 40 µmol L^{-1}. CDOM absorption was measured using a Shimadzu 2401PC spectrophotometer with 1 cm quartz cuvette over the spectral range from 200 to 800 nm with 1 nm intervals. Ultrapure water served as the blank for all samples. Excitation-emission matrices (EEMs) of fluorescent DOM (FDOM) were measured and corrected as in Asmala et al., (2018). For assessing the terrestrial signature of the porewater DOM, fluorescence peaks (peaks A, C, M, and T; Coble, 1996), humification index (HIX; Zsolnay et al., 1999) and biological index (BIX; Huguet et al., 2009) were calculated from the measured and corrected EEMs. Processing of the EEMs was done using the eemR package for R software (Massicotte, 2018).

2.3 Sedimentary nitrogen process rates

Samples for benthic nitrate reduction rate measurements (n=8 per sampling station) were collected into acrylic cores (Ø 2.3 cm, length 15 cm), which were pushed gently into the sediment so that 1/3 of each core was filled with sediment and the rest with overlying water, capped and placed in a water

6

185 bath at *in situ* temperature. The four cores were immediately enriched with ^{15}N-labelled nitrate to a

186 final concentration of 100 µM ^{15}N-NO$_3^-$ (K^{15}NO$_3$ Sigma Aldrich, 98% ^{15}N-atm), closed and incubated

187 under stirring at *in situ* temperature in dark for 3-4 h. Enrichment with 200 µM ^{15}N-NH$_4^+$ (^{15}NH$_4$Cl

188 Cambridge Isotope Laboratories, 99% ^{15}N-atm; 4 replicate cores) was used to exclude anammox and

189 measure nitrification (data not shown). After incubation, sediment and overlying water in the samples

190 were mixed and 12 mL subsamples were transferred into gas-tight glass vials (Labco Exetainer model

191 739W) with 0.5 mL ZnCl$_2$ (100 % w/v, Merck) after a brief sediment settling period. Isotopic

192 composition of N$_2$ and N$_2$O was analysed with a TraceGas preconcentrator system interfaced with an

193 IsoPrime 100 continuous flow isotope ratio mass spectrometer (CF-IRMS; Isoprime Ltd, Cheadle

194 Hulme, UK) at the Department of Environmental Sciences, University of Jyväskylä, Finland as in

195 Hellemann et al., (2017). The detection limits were 320 nmol L^{-1} for ^{29}N$_2$, 11 nmol L^{-1} for ^{30}N$_2$, 397 pmol

196 L^{-1} for ^{45}N$_2$O, and 322 pmol L^{-1} for ^{46}N$_2$O.

197 The remaining ^{15}NO$_3^-$-enriched slurry was mixed again, and 20 mL samples for ^{15}NH$_4^+$ analysis were

198 collected into 50 mL centrifuge tubes, treated with 1 mL of ZnCl$_2$, and frozen immediately. Before

199 ^{15}NH$_4^+$ analysis, NH$_4^+$ attached to the sediment particles was desorbed using KCl extraction. The

200 isotopic composition of NH$_4^+$ in the samples was analyzed after conversion to N$_2$ using alkaline

201 hypobromite iodine solution (Risgaard-Petersen et al., 1995) as in Hellemann et al., (2020). A standard

202 series of ^{15}NH$_4^+$ (5; 10; 15 µM, 5% ^{15}N-atm from ^{15}NH$_4$Cl Cambridge Isotope Laboratories, 98% ^{15}N-atm)

203 was prepared, treated and analyzed parallel with samples to calculate conversion efficiency and ^{15}N

204 recovery, which was > 85 %.

205 The N$_2$ and N$_2$O producing denitrification rates were calculated from the production rates of ^{29}N$_2$, ^{30}N$_2$

206 and ^{45}N$_2$O, ^{46}N$_2$O), and partitioned to denitrification based on water column nitrate (D$_w$) and coupled

207 nitrification-denitrification (D$_n$) (Nielsen, 1992). DNRA rates were calculated from the production rates

208 of ^{15}NH$_4^+$ and the production rates of ^{29}N$_2$, ^{30}N$_2$ and ^{45}N$_2$O, ^{46}N$_2$O in the same incubation cores

209 according to Christensen et al., (2000). It was assumed that DNRA takes place in the same layers as

210 denitrification, meaning that the ^{15}N labeling of NO$_3^-$ reduced to ammonia equals the ^{15}N labeling of

211 NO$_3^-$ reduced to N$_2$/N$_2$O. Total N$_2$ production (∑N$_2$) was calculated as ∑N$_2$ = D$_w$_N$_2$ + D$_n$_N$_2$ and total

212 N$_2$O production (∑N$_2$O) as ∑N$_2$O = D$_w$_N$_2$O + D$_n$_N$_2$O. The total denitrification was then defined as ∑N$_2$

213 + ∑N$_2$O and total nitrate reduction as ∑N$_2$ + ∑N$_2$O + DNRA. The hourly rates were scaled to day by

214 multiplying with 24h. The N$_2$O produced in coupled nitrification-denitrification was divided into the

215 rate of N$_2$O produced in the nitrification stage and the denitrification stage of the coupled nitrification-

216 denitrification according to Dong et al., (2006).

217 **2.4   Statistical analysis**

218   The data analysis was conducted using R (version 3.6.3; R Core Team, 2020). The differences in the

219   porewater DOM characteristics, and N processes between estuary and offshore archipelago region

220   were examined with one-way ANOVA, or if the assumptions on the normality and equal variances

221   were not met, with Mann-Whitney U test. The relationship between DOM variables and N processes

222   were examined with Pearson correlation analysis, and relative DNRA (%DNRA) and N_2O (%N_2O) and

223   DOC and bioavailable carbon fraction (protein-like DOM fluorescence) were further examined with

224   linear regression.

3   Results

225

3.1   Hydrography

226

227   In both estuary and offshore archipelago, the water column was well oxygenated during the sampling

228   campaigns despite being stratified, with a thermocline present at all stations between 3.5-10 m depth

229   (Table 1; Suppl. Fig. 1). At the estuary stations, closer to the direct influence of the Mustionjoki River,

230   a pronounced halocline was present (Suppl. Fig. 1).

231   Table 1. Temperature (T), salinity, oxygen concentration (O_2), and DIN concentrations (NO_x^-, NH_4^+) in

232   near-bottom water and sediment C:N at the estuary and offshore archipelago sampling stations.

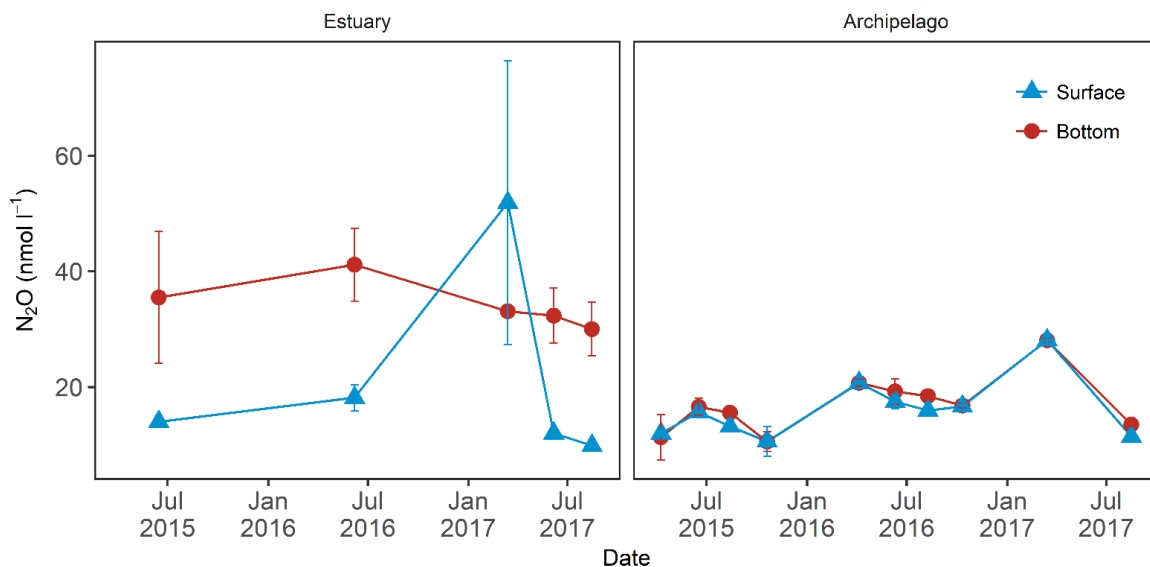|	Station	Sampling time	T °C	salinity	O_2 µM	NO_x^- µM	NH_4^+ µM	C:N
Estuary	P1	June 2017	5.8	4.0	234	11.1	0.7	18.7
	P4	June 2017	3.3	5.1	236	13.0	1.5	12.4
	P1	August 2017	13.8	3.3	155	1.7	3.2	21.6
	P4	August 2017	4.7	5.0	126	14.1	6.1	12.7
Offshore archipelago	P10	August 2017	10.1	6.2	176	1.6	5.8	11.2
	STF	August 2017	8.8	6.4	216	1.4	4.0	10.1

233

3.2   Dissolved inorganic nitrogen and nitrous oxide

234

235   The near-bottom combined nitrite+nitrate (NO_x^-) concentrations decreased as expected from near-

236   shore estuary to offshore archipelago stations. At the estuary stations P1 and P4, near-bottom NO_x^-

concentrations varied between 3-14 µM (Table 1; Suppl. Fig. 2). Near-bottom NO_x^- concentrations were consistently low (≤ 1.6 µM) at the offshore archipelago stations P10 and STF. Near-bottom ammonium (NH_4^+) concentrations (1-6 µM) were similar at all sampling stations. Dissolved nitrous oxide (N_2O) concentrations were consistently high (25-50 nM at P4, Fig. 2) below the halocline in the estuary. Surface waters at the offshore archipelago stations, P4 and STF, and deeper waters at STF, had lower N_2O concentrations (10-30 nM), except for a high value in the surface waters of P4 under ice cover in March 2017.

Figure 2. Nitrous oxide (N_2O) concentration in water column above (blue triangles) and below halocline (red circles) between April 2015 and August 2017 at the near-shore estuary (station P4) and offshore archipelago (station STF) stations. Points indicate mean value and error bars ± 1 standard deviation. Number of observations per each mean value in the figure ranges between 3 and 24, the median number of observations being 10.

3.3   Organic carbon source proxies

All the sampled sediments were muddy, with surface (0-1 cm) porosities ranging from 0.94 to 0.97. Sediment C:N ratio decreased from the estuary (16 ± 5) to the offshore archipelago stations (11 ± 1) (Table 1). The amount of bulk dissolved organic matter in the porewater, as indicated by the DOC concentration, was almost twice as high at the estuary stations as at the offshore archipelago stations (Fig. 3a). The ratio (mean ± SD) between DOC concentrations in the uppermost sediment layer (0-1 cm) and near bottom NO_x (DOC:NO_x^-) was 2.5 ± 2.9 at the estuary stations and 4.8 ± 1.3 at the offshore archipelago stations. Organic matter characteristics were on average more terrestrial-like at the estuary than at the offshore archipelago stations (one-way ANOVA, $p < 0.05$), as indicated by optical proxies: higher CDOM absorption at 254 nm ($a_{(CDOM254)}$), DOC-specific UV absorbance (SUVA$_{254}$), humic- and protein-like DOM fluorescence (peak C and T, respectively) and higher humification index (HIX).

9

Also, at the offshore archipelago stations, UV absorption slope ($S_{275-295}$) and biological index (BIX) were higher than at the estuary stations ($p < 0.05$; Fig. 3), indicating higher contribution of autochthonous bioavailable carbon with smaller molecular size.

3.4 Nitrogen transformation rates in estuary and offshore archipelago sediments

All nitrate reduction rates varied substantially between the sampling stations, as both the highest and lowest rates were measured at the estuarine stations (Fig. 4, Suppl. Fig. 3). Total denitrification ($\sum N_2 + \sum N_2O$) rates and total nitrate reduction ($\sum N_2 + \sum N_2O + DNRA$) rates did not differ significantly between the estuary and offshore archipelago stations (Mann-Whitney U test, $p > 0.05$, Fig. 4, Suppl. Fig. 3). No anammox was detected (data not shown). Denitrification rates based on water column nitrate ($D_w\_N_2$, $D_w\_N_2O$) were higher at the estuary stations ($D_w\_N_2$: one-way ANOVA, $p = 0.004$; $D_w\_N_2O$: $p < 0.001$), but the coupled nitrification-denitrification process rates ($D_n\_N_2$, $D_n\_N_2O$) were dominant and equal between the estuary and offshore archipelago stations ($p > 0.05$, Fig. 4, Suppl. Fig. 3). Similarly, DNRA rates based on water column nitrate ($DNRA_w$) were higher at the estuary stations ($p = 0.006$), while total DNRA rates ($p = 0.024$) and the proportion of DNRA of total nitrate reduction (%DNRA; $p = 0.03$) and nitrification-fed DNRA ($DNRA_n$; $p = 0.003$) rates were higher at the offshore archipelago stations (Fig. 5, Suppl. Fig. 3). The proportion of N_2O produced in nitrate reduction (%N_2O) as well as the proportion of N_2O produced from the denitrification stage of coupled nitrification-denitrification were higher at the estuary stations than at the offshore archipelago stations (%N_2O: $p < 0.001$, %N_2O from denitrification: $p = 0.006$), being especially high at P4 in August (Fig. 5). Significant relationships between organic carbon characteristics (source proxies) and both %DNRA (decreasing with higher terrestrial OM share) and %N_2O (increasing with higher terrestrial OM share) were observed (Suppl. Table 1), while no relationship was found with total denitrification rates. Notably, the variance of either %DNRA or %N_2O was not explained by bulk carbon concentration (DOC) (Fig. 6a–b). Rather, protein-like DOM fluorescence (a common proxy for biologically labile organic carbon) had a strong negative relationship with %DNRA and strong positive relationship with %N_2O (Fig. 6c–d).

Figure 3. Porewater (0–1 cm) DOM quantity and quality characteristics at the estuary stations in June (left orange bar, n = 6) and August (right orange bar, n = 6) and at the offshore archipelago stations in August (n = 6): a) dissolved organic carbon (DOC), b) CDOM absorption coefficient at 254 nm ($a_{(CDOM254)}$, c) humic-like DOM fluorescence (Peak C), d) protein-like DOM fluorescence (Peak T), e) CDOM spectral slope between 275–295 nm ($S_{275-295}$), f) DOC-specific UV absorbance at 254 nm ($SUVA_{254}$), g) humification index (HIX) and h) biological index (BIX). Mean values ± standard deviation for estuary and offshore archipelago groups are also given. The two groups are significantly different for each variable (one-way ANOVA, $p < 0.05$).
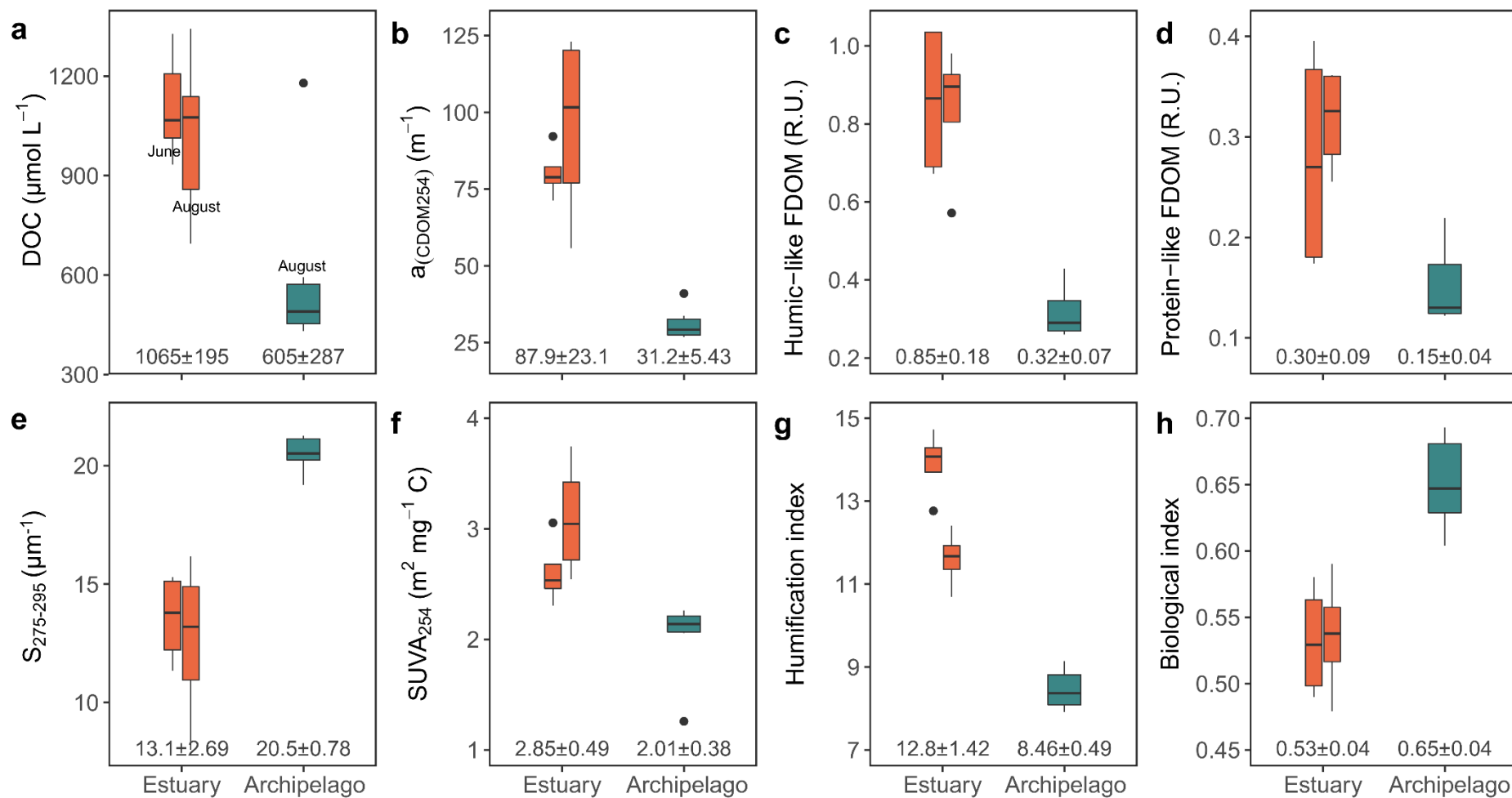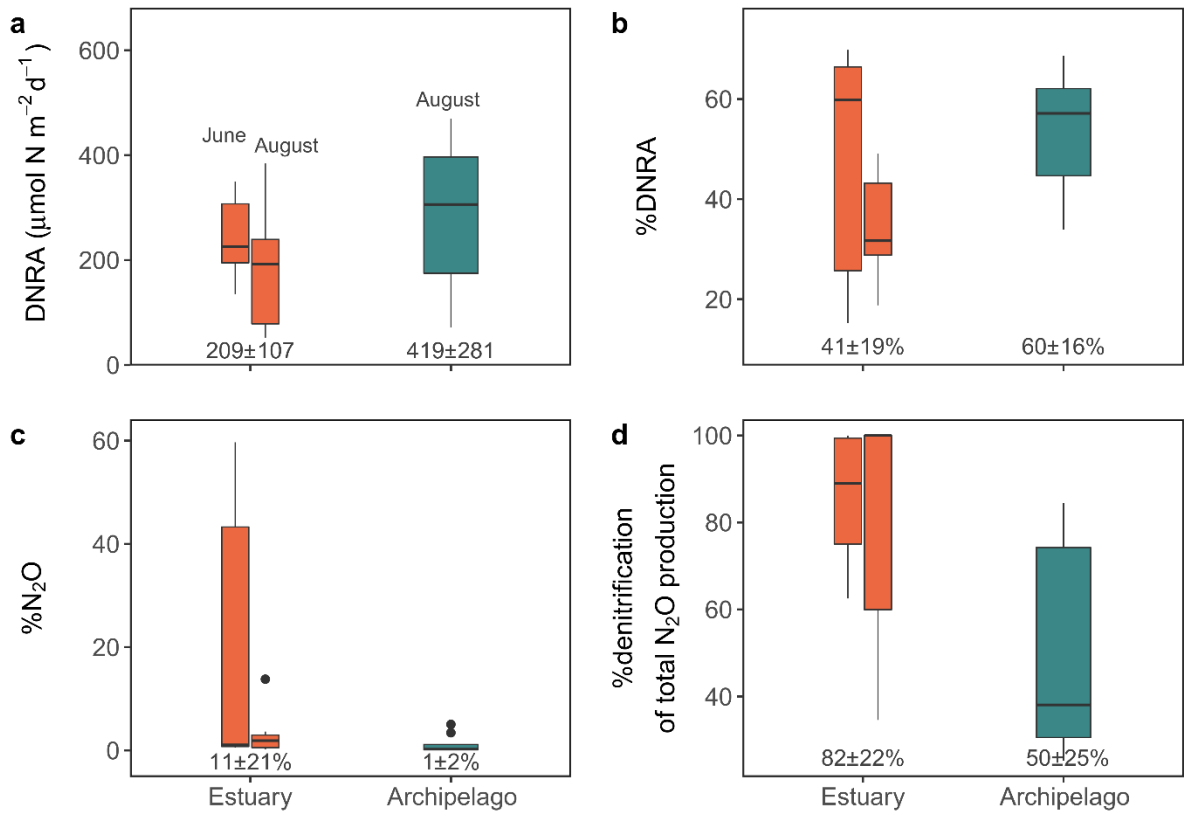
Figure 4. DNRA and denitrification rates at the estuary (P1, P4) and offshore archipelago (P10, STF) stations. D_w denotes water column nitrate based process and D_n process based on the nitrate produced through sediment nitrification. Bars represent mean values ± standard error for four sediment core replicates.
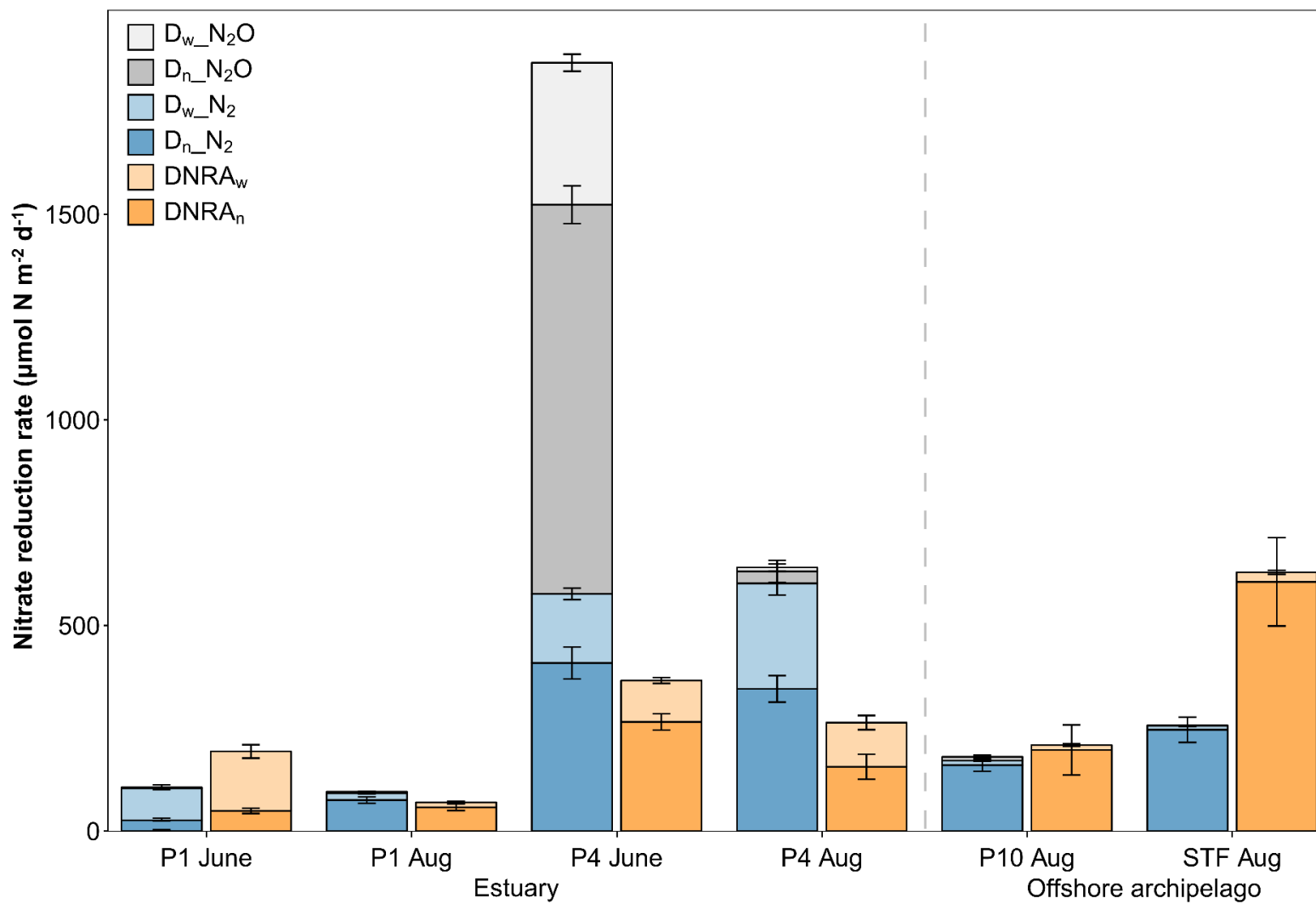
Figure 5. Differences in the a) absolute and b) relative rates of DNRA, and the proportion of N_2O of c) total nitrate reduction, and d) originating from denitrification stage of total N_2O production during coupled nitrification-denitrification process between the estuary stations in June (left orange bar, n = 8) and August (right orange bar, n = 8) and at the offshore archipelago stations in August (n = 8). Mean values ± standard deviation for estuary and offshore archipelago groups are given. The two groups are significantly different for each variable (one-way ANOVA/Mann-Whitney U test, $p < 0.05$).

Figure 6. Relationships between dissolved organic carbon (DOC) and relative a) DNRA and b) N_2O production, and between bioavailable organic matter fraction (protein-like fluorescence; peak T) and relative c) DNRA and d) N_2O production at the estuary and offshore archipelago stations. The linear regression equations of the significant ($p < 0.05$) relationships only are presented.
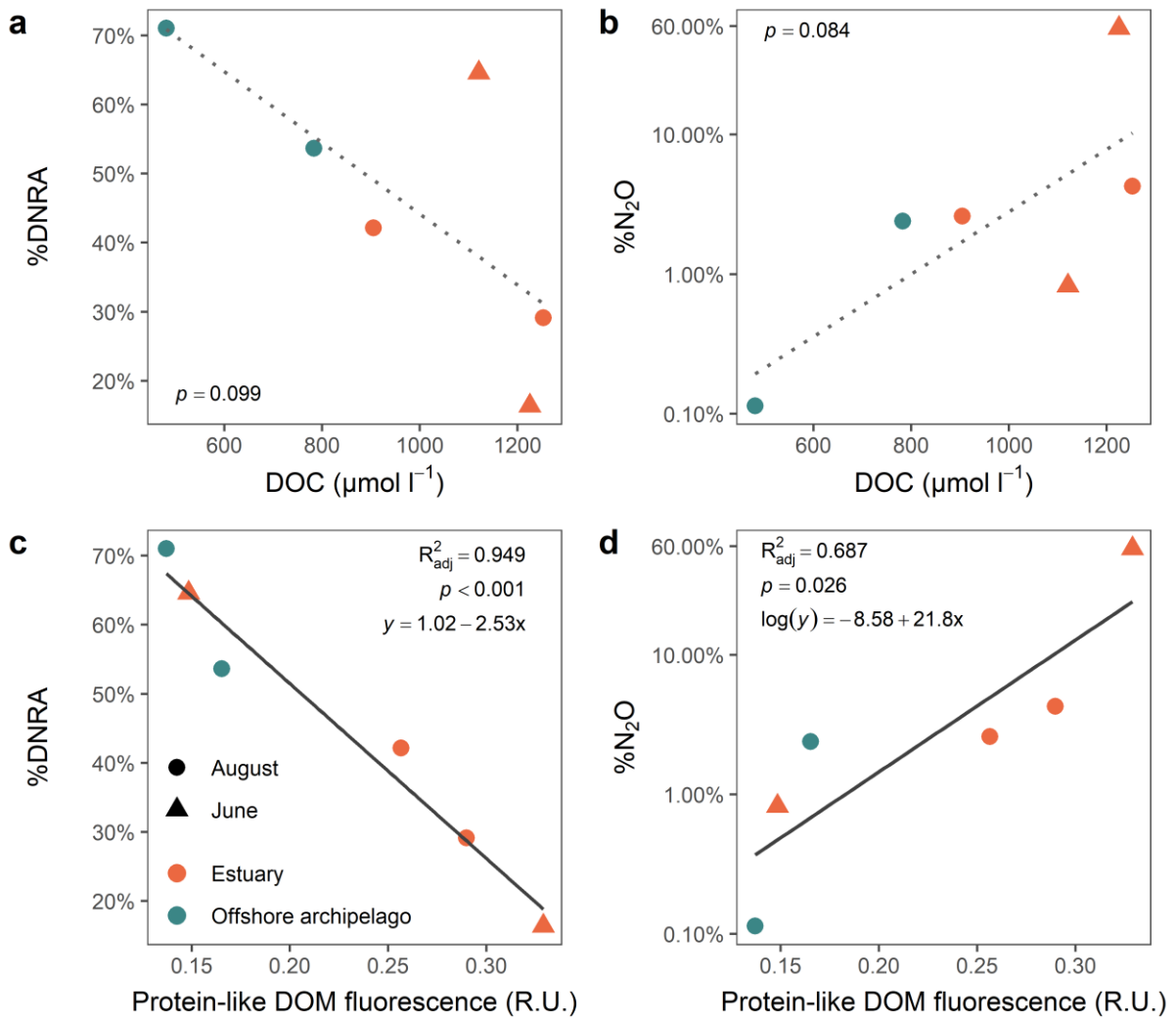
4   Discussion

Our results show that the dominant microbial nitrate reduction process switched from N-removing denitrification to N-recycling DNRA when moving from the terrestrially-dominated estuary to offshore archipelago region. This can be explained by changes in both DIN concentrations and organic carbon bioavailability. As expected, nitrate concentrations were generally higher at the estuarine than at the offshore archipelago stations, due to the diminishing impact of high-DIN riverine water (Asmala et al., 2017). In parallel, we observed strong contrasts in the DOM characteristics between estuary and offshore archipelago. High humic-like fluorescence, humification index and $SUVA_{254}$ in porewater DOM at the estuarine stations indicate a pronounced terrestrial contribution to the DOM pool (Asmala et al., 2013). These proxies suggest low DOM bioavailability in these areas, while high $S_{275-295}$ and BIX values at the offshore archipelago stations indicate a higher contribution of recently produced autochthonous, likely more bioavailable DOM (Lee et al., 2018). A similar gradient in the source of sedimentary particulate OM was observed by Jilbert et al., (2018), where sedimentary N:C values of 0.05-0.06 (C:N of 17-20) observed in the estuary indicated a higher contribution of terrestrially sourced material, while in the offshore region, the N:C of 0.13-0.14 (C:N of 7-8) reflected the dominance of phytoplankton-derived material.

In previous studies, denitrification has been shown to decrease with decreasing water-column nitrate concentrations in the coastal Baltic Sea (Asmala et al., 2017). Our data show that rates of all nitrate reduction processes using water column nitrate ($D_w\_N_2$, $D_w\_N_2O$, $DNRA_w$) decrease from estuary to offshore archipelago (Suppl. Fig. 3). However, because total nitrate reduction was mainly based on the nitrate provided through nitrification rather than water column nitrate, total nitrate reduction rates ($\sum N_2 + \sum N_2O + DNRA$) were not significantly different between estuary and offshore archipelago stations. We suggest that the low amount of bioavailable carbon was limiting denitrification in the estuary, whereas decreasing nitrate availability started to limit the process offshore archipelago. The low bioavailable organic carbon-to-nitrate ratio at the estuarine stations was reflected in the higher denitrification-to-DNRA ratio, whereas DNRA dominated nitrate reduction under high bioavailable carbon-to-nitrate ratio at the offshore archipelago stations. A preference of the sediment microbial community for DNRA under nitrate-limited conditions has previously been explained in terms of the efficiency with which DNRA makes use of nitrate as an electron acceptor, with a higher rate of electron transfer per mole of N reduced despite the higher free energy yield of denitrification (Algar and Vallino, 2014). Interestingly, the DOM characteristics was directly related to N processes, while the amount of bulk organic carbon (as indicated by the porewater DOC concentration) was not (Fig. 6). We acknowledge that several alternative factors may influence rates and pathways of nitrate

reduction processes in coastal sediments. For instance, the presence of hydrogen sulfide (H_2S) close to the sediment-water interface promotes %DNRA (Plummer et al., 2015). However, upper-sediment sulfide concentrations in the range of 1–3 mM are required for a clear impact on N processes, while sulfide in the upper sediments of our study area were consistently < 0.1 mM (Jilbert et al., 2018). These low concentrations result from the titrating effect of sedimentary Fe oxides in the coastal Baltic Sea, suggesting that sulfide is a minor driver of the observed changes in %DNRA in our dataset. Furthermore, the presence of abundant Fe oxides producing Fe^{2+}, an alternative electron donor, may promote DNRA (Kessler et al., 2018; Robertson et al., 2016). Again, our study area shows only mild enrichments of porewater Fe^{2+} in the upper sediments (up to 0.2 mM, Jilbert et al., 2018) in comparison to the sites studied by Robertson et al., (2016) (up to 0.8 mM), decreasing the potential significance of Fe. The anomalously high rates of DNRA at P1 in June may however relate to porewater Fe^{2+}, since this is the most Fe-rich of our sampling stations (see Station A in Jilbert et al., 2018).

In addition, our results demonstrate that the overall difference in potential organic carbon bioavailability between estuary and offshore archipelago regions is likely to influence the end-product of denitrification. At the near-shore estuarine stations, denitrification produced high proportions of N_2O (1-58% of total nitrate reduction; 3-1230 µM N m^{-2} d^{-1}). This result implies that nitrate was preferred over N_2O as an electron acceptor under conditions of high nitrate to bioavailable carbon the nitrate-replete conditions of the estuary (Richardson et al., 2009), allowing N_2O to accumulate in bottom waters. In contrast, the share of N_2O in denitrification was lower in the offshore archipelago stations (0.1-2%, 1-9 µmol N m^{-2} d^{-1}), where the bulk carbon concentrations were low but the contribution of bioavailable autochthonous carbon to the carbon pool was high and nitrate concentration low. In accordance, N_2O concentrations in the bulk water column samples collected between 2015 and 2017 were higher at the estuarine stations than in the offshore archipelago, agreeing with the previous results in coastal environments with high freshwater impact and fluctuating environmental conditions (e.g. Foster and Fulweiler, 2016; Nielsen et al., 2009; Silvennoinen et al., 2008). While part of the accumulated N_2O can originate from nitrification or coupled nitrification-denitrification (Foster and Fulweiler, 2016), we measured rather equal rates of sediment nitrification at the estuary and offshore archipelago stations (estuary: 841±378, offshore archipelago: 1089±193 µmol N m^{-2} d^{-1}; data not shown), arguing against an important role for nitrification in N_2O production in the estuary. Furthermore, our data show that N_2O produced in coupled nitrification-denitrification was mainly derived from denitrification. Although part of the water-column N_2O pool in the estuary is likely advected with riverine water (Bange et al., 1998), the majority appears to derive from sediment processes, since N_2O concentrations were generally higher in the bottom water than at the surface (Fig. 2).

Coastal systems are considered as important nutrient filters, reducing N loading from catchment areas towards the open sea. Although our results confirm that the main N removal process in the studied coastal environment is N_2-producing heterotrophic denitrification, they also highlight the importance of N-recycling DNRA. In the outer offshore archipelago region with decreasing influence of riverine water, DNRA can produce substantial amounts of bioavailable ammonium, enhancing the N recycling between sediments and surface water, especially in summer with the highest autochthonous biomass production and sedimentation. Intensifying eutrophication increases bioavailable carbon availability through higher algal biomass production, which in turn may promote DNRA and increase the role of estuaries as hotspots for N recycling, over N removal. This phenomenon has already been observed in some eutrophied systems (Bernard et al., 2015; Song et al., 2014), and could delay the recovery of water quality of the open sea in the Baltic Sea region.

The future role of eutrophic coastal systems as sources of N_2O to the atmosphere depends on the balance of N processes in coastal sediments. In systems such as Pohjanpitäjänlahti, the DIN pool of the estuary is dominated by nitrate, favouring production of N_2O during denitrification under nitrate-replete conditions. Hence, further increases in nutrient loading to this system is likely to enhance N_2O-producing denitrification, especially under scenarios of increased annual runoff and higher summer temperature, which will enhance stratification and hypoxia throughout the Baltic Sea (Meier et al., 2011), contributing to the predicted rise in emissions of this greenhouse gas in the future (Murray et al., 2015). Our results highlight the need to consider the intricate balance of processes in the nitrogen cycle along coastal gradients, especially in relation to organic carbon characteristics. Also their spatial variation and temporal evolution needs to be further clarified in order to properly understand the role of coastal ecosystems as filters of land-to-sea transfer of N.

5 Acknowledgements

6 References

Algar, C.K., Vallino, J.J., 2014. Predicting microbial nitrate reduction pathways in coastal sediments. Aquat. Microb. Ecol. 71, 223–238. https://doi.org/10.3354/ame01678

Asmala, E., Autio, R., Kaartokallio, H., Pitkänen, L., Stedmon, C.A., Thomas, D.N., 2013. Bioavailability of riverine dissolved organic matter in three Baltic Sea estuaries and the effect of catchment

410   land use. Biogeosciences 10, 6969–6986. https://doi.org/10.5194/bg-10-6969-2013

411   Asmala, E., Carstensen, J., Conley, D.J., Slomp, C.P., Stadmark, J., Voss, M., 2017. Efficiency of the

412   coastal filter: Nitrogen and phosphorus removal in the Baltic Sea. Limnol. Oceanogr. 62, S222–

413   S238. https://doi.org/10.1002/lno.10644

414   Asmala, E., Haraguchi, L., Markager, S., Massicotte, P., Riemann, B., Staehr, P.A., Carstensen, J., 2018.

415   Eutrophication Leads to Accumulation of Recalcitrant Autochthonous Organic Matter in Coastal

416   Environment. Global Biogeochem. Cycles 32, 1673–1687.

417   https://doi.org/10.1029/2017GB005848

418   Bange, H.W., Dahlke, S., Ramesh, R., Meyer-Reil, L.A., Rapsomanikis, S., Andreae, M.O., 1998.

419   Seasonal study of methane and nitrous oxide in the coastal waters of the southern Baltic Sea.

420   Estuar. Coast. Shelf Sci. 47, 807–817. https://doi.org/10.1006/ecss.1998.0397

421   Barnes, R.T., Smith, R.L., Aiken, G.R., 2012. Linkages between denitrification and dissolved organic

422   matter quality, Boulder Creek watershed, Colorado. J. Geophys. Res. Biogeosciences 117, 1–14.

423   https://doi.org/10.1029/2011JG001749

424   Bernard, R.J., Mortazavi, B., Kleinhuizen, A.A., 2015. Dissimilatory nitrate reduction to ammonium

425   (DNRA) seasonally dominates NO_3^- reduction pathways in an anthropogenically impacted sub-

426   tropical coastal lagoon. Biogeochemistry 125, 47–64. https://doi.org/10.1007/s10533-015-

427   0111-6

428   Bonaglia, S., Deutsch, B., Bartoli, M., Marchant, H.K., Brüchert, V., 2014. Seasonal oxygen, nitrogen

429   and phosphorus benthic cycling along an impacted Baltic Sea estuary: Regulation and spatial

430   patterns. Biogeochemistry 119, 139–160. https://doi.org/10.1007/s10533-014-9953-6

431   Bouwman, A.F., Bierkens, M.F.P., Griffioen, J., Hefting, M.M., Middelburg, J.J., Middelkoop, H.,

432   Slomp, C.P., 2013. Nutrient dynamics, transfer and retention along the aquatic continuum from

433   land to ocean: Towards integration of ecological and biogeochemical models. Biogeosciences

434   10, 1–23. https://doi.org/10.5194/bg-10-1-2013

435   Burdige, D.J., 2006. Geochemistry of Marine Sediments, 1st ed. Princeton Univ. Press, Princeton.

436   Carlson, H.K., Lui, L.M., Price, M.N., Kazakov, A.E., Carr, A. V., Kuehl, J. V., Owens, T.K., Nielsen, T.,

437   Arkin, A.P., Deutschbauer, A.M., 2020. Selective carbon sources influence the end-products of

438   microbial nitrate respiration. ISME J. https://doi.org/10.1038/s41396-020-0666-7

439   Christensen, P.B., Rysgaard, S., Sloth, N.P., Dalsgaard, T., Schwærter, S., 2000. Sediment

440   mineralization, nutrient fluxes, denitrification and dissimilatory nitrate reduction to ammonium

441   in an estuarine fjord with sea cage trout farms. Aquat. Microb. Ecol. 21, 73–84.

442   https://doi.org/10.3354/ame021073

443 Coble, P.G., 1996. Characterization of marine and terrestrial DOM in seawater using excitation-

444   emission matrix spectroscopy. Mar. Chem. 51, 325–346. https://doi.org/10.1016/0304-

445   4203(95)00062-3

446 Dong, L.F., Nedwell, D.B., Stott, A., 2006. Sources of nitrogen used for denitrification and nitrous

447   oxide formation in sediments of the hypernutrified Colne, the nutrified Humber, and the

448   oligotrophic Conwy estuaries, United Kingdom. Limnol. Oceanogr. 51, 545–557.

449   https://doi.org/10.4319/lo.2006.51.1_part_2.0545

450 Fellman, J.B., Petrone, K.C., Grierson, P.F., 2011. Source, biogeochemical cycling, and fluorescence

451   characteristics of dissolved organic matter in an agro-urban estuary. Limnol. Oceanogr. 56,

452   243–256. https://doi.org/10.4319/lo.2011.56.1.0243

453 Foster, S.Q., Fulweiler, R.W., 2016. Sediment nitrous oxide fluxes are dominated by uptake in a

454   temperate estuary. Front. Mar. Sci. 3, 1–13. https://doi.org/10.3389/fmars.2016.00040

455 Giblin, A.E., Tobias, C.R., Song, B., Weston, N., Banta, G.T., Rivera-Monroy, V.H., 2013. The

456   importance of dissimilatory nitrate reduction to ammonium (DNRA) in the nitrogen cycle of

457   coastal ecosystems. Oceanography 26, 124–131. https://doi.org/10.5670/oceanog.2013.54

458 Goñi, M.A., Teixeira, M.J., Perkeya, D.W., 2003. Sources and distribution of organic matter in a river-

459   dominated estuary (Winyah Bay, SC, USA). Estuar. Coast. Shelf Sci. 57, 1023–1048.

460   https://doi.org/10.1016/S0272-7714(03)00008-8

461 Hardison, A.K., Algar, C.K., Giblin, A.E., Rich, J.J., 2015. Influence of organic carbon and nitrate

462   loading on partitioning between dissimilatory nitrate reduction to ammonium (DNRA) and N2

463   production. Geochim. Cosmochim. Acta 164, 146–160.

464   https://doi.org/10.1016/j.gca.2015.04.049

465 Heiskanen, A.S., Kononen, K., 1994. Sedimentation of vernal and late summer phytoplankton

466   communities in the coastal Baltic Sea. Arch. fur Hydrobiol. 131, 175–198.

467 Hellemann, D., Tallberg, P., Aalto, S.L., Bartoli, M., Hietanen, S., 2020. Seasonal cycle of benthic

468   denitrification and DNRA in the aphotic coastal zone, northern Baltic Sea. Mar. Ecol. Prog. Ser.

469   637, 15–28.

470 Hellemann, D., Tallberg, P., Bartl, I., Voss, M., Hietanen, S., 2017. Denitrification in an oligotrophic

471   estuary: A delayed sink for riverine nitrate. Mar. Ecol. Prog. Ser. 583, 63–80.

472   https://doi.org/10.3354/meps12359

473   Hietanen, S., 2007. Anaerobic ammonium oxidation (anammox) in sediments of the Gulf of Finland.
474   Aquat. Microb. Ecol. 48, 197–205. https://doi.org/10.3354/ame048197

475   Hietanen, S., Kuparinen, J., 2008. Seasonal and short-term variation in denitrification and anammox
476   at a coastal station on the Gulf of Finland, Baltic Sea. Hydrobiologia 596, 67–77.
477   https://doi.org/10.1007/s10750-007-9058-5

478   Huguet, A., Vacher, L., Relexans, S., Saubusse, S., Froidefond, J.M., Parlanti, E., 2009. Properties of
479   fluorescent dissolved organic matter in the Gironde Estuary. Org. Geochem. 40, 706–719.
480   https://doi.org/10.1016/j.orggeochem.2009.03.002

481   Jilbert, T., Asmala, E., Schröder, C., Tiihonen, R., Myllykangas, J.P., Virtasalo, J.J., Kotilainen, A.,
482   Peltola, P., Ekholm, P., Hietanen, S., 2018. Impacts of flocculation on the distribution and
483   diagenesis of iron in boreal estuarine sediments. Biogeosciences 15, 1243–1271.
484   https://doi.org/10.5194/bg-15-1243-2018

485   Kessler, A.J., Roberts, K.L., Bissett, A., Cook, P.L.M., 2018. Biogeochemical Controls on the Relative
486   Importance of Denitrification and Dissimilatory Nitrate Reduction to Ammonium in Estuaries.
487   Global Biogeochem. Cycles 32, 1045–1057. https://doi.org/10.1029/2018GB005908

488   Kraft, B., Tegetmeyer, H.E., Sharma, R., Klotz, M.G., Ferdelman, T.G., Hettich, R.L., Geelhoed, J.S.,
489   Strous, M., 2014. The environmental controls that govern the end product of bacterial nitrate
490   respiration. Science (80-.). 345, 676–679. https://doi.org/10.1126/science.1254070

491   Lee, M.H., Osburn, C.L., Shin, K.H., Hur, J., 2018. New insight into the applicability of spectroscopic
492   indices for dissolved organic matter (DOM) source discrimination in aquatic systems affected
493   by biogeochemical processes. Water Res. 147, 164–176.
494   https://doi.org/10.1016/j.watres.2018.09.048

495   Malve, O., Virtanen, M., Villa, L., Karonen, M., Aakerla, H., Heiskanen, A.S., Lappalainen, K.M.,
496   Holmberg, R., 2000. Artificial oxygenation experiment in hypolimnion of Pojo Bay estuary in
497   1995 and 1996: Factors regulating estuary circulation and oxygen and salt balances. Finnish
498   Environ. 377, 1-163 (In Finnish with English summary).

499   Massicotte, P., 2018. eemR: Tools for Pre-Processing Emission-Excitation-Matrix (EEM) Fluorescence
500   Data. R package version 1.0.1. https://CRAN.R-project.org/package=eemR.

501   Mattsson, T., Kortelainen, P., Räike, A., 2005. Export of DOM from boreal catchments: Impacts of
502   land use cover and climate. Biogeochemistry 76, 373–394. https://doi.org/10.1007/s10533-

503   005-6897-x

504 Meier, H.E.M., Andersson, H.C., Eilola, K., Gustafsson, B.G., Kuznetsov, I., Mller-Karulis, B., Neumann,
505   T., Savchuk, O.P., 2011. Hypoxia in future climates: A model ensemble study for the Baltic Sea.
506   Geophys. Res. Lett. 38, 1–6. https://doi.org/10.1029/2011GL049929

507 Murphy, K.R., Stedmon, C.A., Waite, T.D., Ruiz, G.M., 2008. Distinguishing between terrestrial and
508   autochthonous organic matter sources in marine environments using fluorescence
509   spectroscopy. Mar. Chem. 108, 40–58. https://doi.org/10.1016/j.marchem.2007.10.003

510 Murray, R.H., Erler, D. V., Eyre, B.D., 2015. Nitrous oxide fluxes in estuarine environments: Response
511   to global change. Glob. Chang. Biol. 21, 3219–3245. https://doi.org/10.1111/gcb.12923

512 Myllykangas, J.P., Jilbert, T., Jakobs, G., Rehder, G., Werner, J., Hietanen, S., 2017. Effects of the 2014
513   major Baltic inflow on methane and nitrous oxide dynamics in the water column of the central
514   Baltic Sea. Earth Syst. Dyn. 8, 817–826. https://doi.org/10.5194/esd-8-817-2017

515 Nielsen, L.P., 1992. Denitrification in sediment determined from nitrogen isotope pairing. FEMS
516   Microbiol. Lett. 86, 357–362. https://doi.org/10.1111/j.1574-6968.1992.tb04828.x

517 Nielsen, M., Gieseke, A., De Beer, D., Revsbech, N.P., 2009. Nitrate, nitrite, and nitrous oxide
518   transformations in sediments along a salinity gradient in the Weser Estuary. Aquat. Microb.
519   Ecol. 55, 39–52. https://doi.org/10.3354/ame01275

520 Plummer, P., Tobias, C., Cady, D., 2015. Nitrogen reduction pathways in estuarine sediments:
521   Influences of organic carbon and sulfide. J. Geophys. Res. Biogeosciences 120, 1958–1972.
522   https://doi.org/10.1002/2015JG003004.Received

523 R Core Team, 2020. R: A language and environment for statistical computing.

524 Räike, A., Kortelainen, P., Mattsson, T., Thomas, D.N., 2012. 36year trends in dissolved organic
525   carbon export from Finnish rivers to the Baltic Sea. Sci. Total Environ. 435–436, 188–201.
526   https://doi.org/10.1016/j.scitotenv.2012.06.111

527 Richardson, D., Felgate, H., Watmough, N., Thomson, A., Baggs, E., 2009. Mitigating release of the
528   potent greenhouse gas N2O from the nitrogen cycle - could enzymic regulation hold the key?
529   Trends Biotechnol. 27, 388–397. https://doi.org/10.1016/j.tibtech.2009.03.009

530 Risgaard-Petersen, N., Revsbech, N.P., Rysgaard, S., 1995. Combined microdiffusion-hypobromite
531   oxidation method for determining nitrogen-15 isotope in ammonium. Soil Sci. Soc. Am. J. 59,
532   1077–1080.

533 Robertson, E.K., Roberts, K.L., Burdorf, L.D.W., Cook, P., Thamdrup, B., 2016. Dissimilatory nitrate
534   reduction to ammonium coupled to Fe(II) oxidation in sediments of a periodically hypoxic
535   estuary. Limnol. Oceanogr. 61, 365–381. https://doi.org/10.1002/lno.10220

536 Silvennoinen, H., Liikanen, A., Torssonen, J., Stange, C.F., Martikainen, P.J., 2008. Denitrification and
537   N2O effluxes in the Bothnian Bay (northern Baltic Sea) river sediments as affected by
538   temperature under different oxygen concentrations. Biogeochemistry 88, 63–72.
539   https://doi.org/10.1007/s10533-008-9194-7

540 Song, B., Lisa, J.A., Tobias, C.R., 2014. Linking DNRA community structure and activity in a shallow
541   lagoonal estuarine system. Front. Microbiol. 5, 1–10.
542   https://doi.org/10.3389/fmicb.2014.00460

543 Spencer, R.G.M., Ahad, J.M.E., Baker, A., Cowie, G.L., Ganeshram, R., Upstill-Goddard, R.C., Uher, G.,
544   2007. The estuarine mixing behaviour of peatland derived dissolved organic carbon and its
545   relationship to chromophoric dissolved organic matter in two North Sea estuaries (U.K.).
546   Estuar. Coast. Shelf Sci. 74, 131–144. https://doi.org/10.1016/j.ecss.2007.03.032

547 Stelzer, R.S., Thad Scott, J., Bartsch, L.A., Parr, T.B., 2014. Particulate organic matter quality
548   influences nitrate retention and denitrification in stream sediments: Evidence from a carbon
549   burial experiment. Biogeochemistry 119, 387–402. https://doi.org/10.1007/s10533-014-9975-0

550 Thamdrup, B., Dalsgaard, T., 2002. Production of N2 through anaerobic ammonium oxidation
551   coupled to nitrate reduction in marine sediments. Appl. Environ. Microbiol. 68, 1312–1318.
552   https://doi.org/10.1128/AEM.68.3.1312

553 Zhao, Y., Xia, Y., Li, B., Yan, X., 2014. Influence of environmental factors on net N2 and N2O
554   production in sediment of freshwater rivers. Environ. Sci. Pollut. Res. 21, 9973–9982.
555   https://doi.org/10.1007/s11356-014-2908-6

556 Zsolnay, A., Baigar, E., Jimenez, M., Steinweg, B., Saccomandi, F., 1999. Differentiating with
557   fluorescence spectroscopy the sources of dissolved organic matter in soils subjected to drying.
558   Chemosphere 38, 45–50. https://doi.org/10.1016/S0045-6535(98)00166-0

559